On Fading Margin in Ultrawideband Communications Over Multipath Channels

Enrique René Bastidas-Puga, Fernando Ramírez-Mireles, and David Muñoz-Rodríguez

***Abstract*—This work studies ultra wideband (UWB) communications over multipath residential indoor channels. We study the relationship between the fading margin and the transmitter–receiver separation distance for both the line of sight and the no line of sight scenarios. Impairments such as small scale fading as well as large scale fading are considered. Some implications of the results for UWB indoor network design are discussed.**

***Index Terms*—BER, multipath, PPM, UWB.**

I. Introduction

MULTIPATH fading resistance and high data rate transmission capacity [1]–[3] make ultra wideband (UWB) technology an excellent option for wireless communications in home applications [4] such as wireless TV, or in local area networks to provide access to internet services and to enable multimedia applications [5].

The UWB signals receive their name due to their very wide bandwidth. A signal is defined to be UWB when its bandwidth, measured at the -10 dB points, is greater than 0.2 times its central frequency, or when it is greater than 500 MHz [6].

The literature shows several UWB performance analyses for multipath indoor channels in commercial office buildings [2], [7]–[9]. The work in [2] and [7] analyze M-ary pulse position modulation (PPM) communications with ideal and low complexity Rake receivers, respectively. The work in [9] uses binary PPM data to compare ideal versus reduced complexity Rake receivers, with a statistical multipath channel model from an office building and using a semi-analytical evaluation of bit error rate (BER) similar to the calculation done in [8].

The fading margin (FM) in wireless communications is the average increase in required signal power to provide the same average error probability on fading versus non fading channels [10]. The reduced FM properties in UWB communications over multipath channels have been studied before [2], [8]. In this work we are interested in how this fading margin FM (d) depends on the transmitter–receiver separation distance d [11]. In particular, we analyze the dependence of the received signal variance on the link length. In the analysis we consider the effects of both small scale and large scale fading. We make calculations for both the line-of-sight (LOS) and the no-line-of-sight (NLS) scenarios.

Manuscript received August 16, 2004; revised December 23, 2004.

E. R. Bastidas-Puga is with the Universidad Autónoma de Baja California (UABC), Facultad de Ingeniería, Unidad Universitaria, Mexicali, Baja California, C.P. 21280, México (e-mail: rbastidas@uabc.mx).

F. Ramírez-Mireles is with the Instituto Tecnológico Autónomo de México (ITAM), Col Tizapán San Angel Ciudad de México, D.F., C.P. 01000, México (e-mail: ramirezm@ieee.org).

D. Muñoz-Rodríguez is with the Instituto Tecnológico y de Estudios Superiores de Monterrey (ITESM), Monterrey, N.L., C.P. 64849, México (e-mail: dmunoz@itesm.mx).

Digital Object Identifier 10.1109/TBC.2005.846199

Based on the fading margin results, we provide some guidelines useful for UWB indoor network design.

II. System Model

This analysis uses binary PPM, with a channel model suitable for indoor residential environments [12], as well as a stochastic path loss model designed from the same measurement experiment [13]. The system model is explained in more detail in [14].

A. Signal Description

The PPM signal $s(t)$ is the *received* signal representing a bit. In the absence of noise $s(t)$ can be written as follows [1], [8]

$$s(t) = \sum_{k=0}^{N_s-1} w_s(t - kT_f - \delta_b), \quad b = 0, 1 \tag{1}$$

where δ_b is the shift due to data modulation, k indexes each transmitted pulse, T_f is the allowable time window for each pulse to be transmitted, and N_s represents the number of pulses transmitted per bit b.

Let $w_s(t)$ be the received UWB "pulse" under multipath conditions with duration T_s in the order of 100's of ns, and let $w(t)$ be the received UWB pulse under free space propagation conditions with duration T_w in the order of a few ns; hence $w_s(t)$ is a *spreaded* version of $w(t)$ with $T_s \gg T_w$. In (1) the $s(t)$ is composed of N_s UWB pulses $w_s(t)$, with $T_f > T_s + \delta_b$.

Notice that the multipath profiles are assumed to have a fixed length T_s, long enough to contain the majority of the energy. Also notice that the frame time T_f is chosen to be longer than the duration of the MP profile T_s; hence both inter-pulse and inter-symbol can be neglected.

With a proper Rake receiver configuration [2], [3], the pulse replicas arriving in the receiver with delays larger than the UWB pulse width T_w can be resolved and their energy can be combined to increase the total received energy. Hence, UWB systems are resistant to the deleterious effects of fading caused by dense multipath.

The frequency spectrum of $s(t)$ is

$$S(\omega) = W_s(\omega) \sum_{k=0}^{N_s-1} e^{-j\omega(kT_f+\delta_b)}, \quad b = 0, 1 \tag{2}$$

where

$$W_s(\omega) = W(\omega)H(\omega) \tag{3}$$

is the received pulse frequency spectrum, $W(\omega)$ is the Fourier transform of $w(t)$, and $H(\omega)$ is the Fourier transform of the impulse response of the slowly varying indoor multipath channel.

The energy of $s(t)$ is given by $E_s = N_s E_w$, where

$$E_w = \int_{-\infty}^{\infty} |w_s(t)|^2 \, dt = \frac{1}{2\pi} \int_{-\infty}^{\infty} |W_s(\omega)|^2 \, d\omega$$

is the energy of $w_s(t)$. Both $s(t)$ and $w_s(t)$ have normalized correlation given by

$$\gamma(\tau) = \int_{-\infty}^{\infty} \frac{s(t)s(t-\tau)}{E_s} dt = \int_{-\infty}^{\infty} \frac{w_s(t)w_s(t-\tau)}{E_w} dt$$
$$= \frac{1}{E_w} \frac{1}{2\pi} \int_{-\infty}^{\infty} |W_s(\omega)|^2 e^{j\omega\tau} d\omega,\ \tau \in [-T_w, T_w]$$

since pulses are non overlapping.

B. Channel Frequency Response

In our analysis we use an auto-regressive (AR) statistical channel model [12] obtained by using frequency domain data measured in a propagation experiment in residential environments (over 23 residential homes with different structure, material, age, and clutter) [13]. The AR model accounts for the small scale fading impairments introduced by the multipath environment. The channel frequency response $H(\omega)$ is centered around 5 GHz, and corresponds to the output sequence of an infinite impulse response (IIR) filter. The input to the IIR filter, the initial conditions, and coefficients are all random.

In this analysis we also use the path loss (PL) model for large scale fading impairments developed in [13] with the same experimental data used for the AR model. The PL is a lognormal shadow fading model. For more details about the channel model please see the Appendix.

C. Distance-Dependence

Clearly, the channel response varies as a function of d, e.g., in the AR model the variance of the filter excitation, and the initial conditions are distance-dependant. Obviously, the PL model is distance-dependant. The PL produces frequency-independent variations, and the frequency-dependant variations are given by $H(\omega)$. The reader can easily find expressions for $E_w(d)$ and $\gamma(\delta, d)$ as a function of d.

III. Performance Analysis

In this analysis we consider a Rake receiver perfectly synchronized and matched to the information signal. The received signal contains additive white Gaussian Noise (AWGN) with two-sided power spectral density (PSD) $N_o/2$.

A. Conditioned BER

Let's assume, for the time being, that d and the channel conditions are kept fixed. Using standard communications theory [15], we can calculate the bit error probability for equally likely bits. When a bit 0 is transmitted, the error probability is

$$P_e(d) = Q\left(\sqrt{\mathrm{SNR}_{|b=0}(d)}\right) \tag{4}$$

where [14]

$$\mathrm{SNR}_{|b=0}(d) = \frac{N_s E_w(d)\left(1 - \Re\left\{\gamma(\delta, d)\right\}\right)}{N_0}$$

is the distance-dependant bit signal-to-noise ratio (SNR), $Q(\cdot)$ is the Gaussian tail integral, and $\Re\{\cdot\}$ is the real-part operator. For equally likely bits, the total BER is given by P_e in (4).

B. Averaged BER

Equation (4) gives the BER conditioned on a particular channel realization. To average the BER considering the random channel effects (with a fixed d), we use the same semi-analytical approach described in [8] to get

$$P_{\mathrm{avg}}\left(\mathrm{SNR}_{\mathrm{avg}}(d)\right) = \mathbf{E}[P_e] \simeq \frac{1}{M} \sum_{i=1}^{M} Q\left(\sqrt{\mathrm{SNR}_i(d)}\right) \tag{5}$$

where $P_{\mathrm{avg}}(\mathrm{SNR}_{\mathrm{avg}}(d))$ is the distance-dependant averaged bit error probability, $\mathrm{SNR}_{\mathrm{avg}}(d)$ is the average receiver SNR, $\mathbf{E}[\cdot]$ is the mean estimator with respect to the random multipath channel, $\mathrm{SNR}_i(d)$ is the SNR at the receiver calculated for each realization, and M is the number of channel realizations.

C. FM, SNR and BER

In this work we analyze $\mathrm{FM}(d)$ as a function of d, while the BER is maintained fixed. For this purpose, we first study how the bit error rate $\mathrm{BER}(d)$ changes as we vary d, while the SNR is maintained fixed (i.e., as d is varied, we increase or decrease the transmitted signal energy to maintain the same average SNR in the receiver). We then use these constant SNR curves to calculate $\mathrm{FM}(d)$.

IV. Simulation and Numerical Results

In this work the basic pulse $w_s(t)$ is the second derivative of a Gaussian pulse [1], [8] multiplied by a complex exponential at 5 GHz, giving a frequency spectrum

$$W(\omega) = \frac{1}{2}\sqrt{\pi}\left[t_0(\omega - \omega_0)\right]^2 \cdot e^{-\left[\frac{t_0}{2}(\omega-\omega_0)\right]^2} \tag{6}$$

where $\omega = 2\pi f$, f is the frequency in Hz, $\omega_0 = 2\pi f_0$, $f_0 = 5$ GHz, and $t_0 = 0.5 \times 10^{-9}$ sec.. (resulting in $T_w \approx 4$ ns). We use orthogonal PPM with $\delta_0 = 0$ and $\delta_1 = 4$ ns, and $T_f > 200$ ns.

The $H(\omega)$ and $W(\omega)$ are obtained for $f = 3.75, \ldots, 6.25$ GHz in 3.125 MHz steps (a total of 801 points). The $H(\omega)$ and PL are obtained for each channel realization using Monte Carlo simulation. The method used for channel model generation is explained in references [12] and [13]. The method used to generate channel realizations according to the model is explained more in depth in the appendix. (For a full description of the computer generation methods see [14]).

From $W(\omega)$ in (6) and every pair $H(\omega)(d)$, $\mathrm{PL}(d)$ we calculate one $\mathrm{SNR}(d)$ value and a corresponding $P_e(d)$ in (4). For

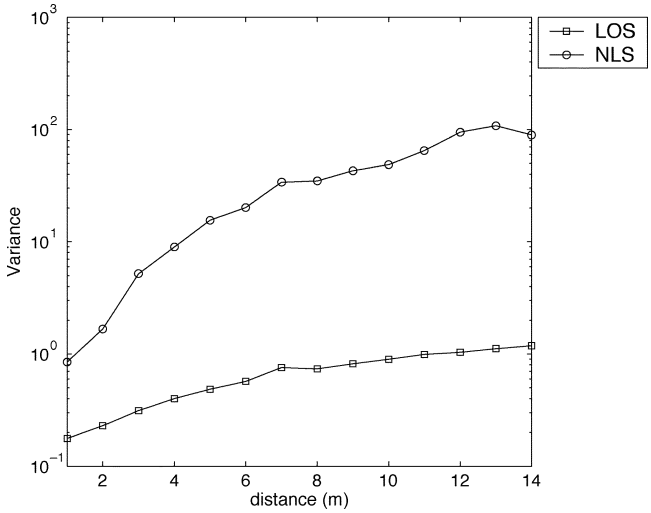

Fig. 1. Received energy variance $\mathrm{VAR}[E_s(d)]$ vs. distance d.

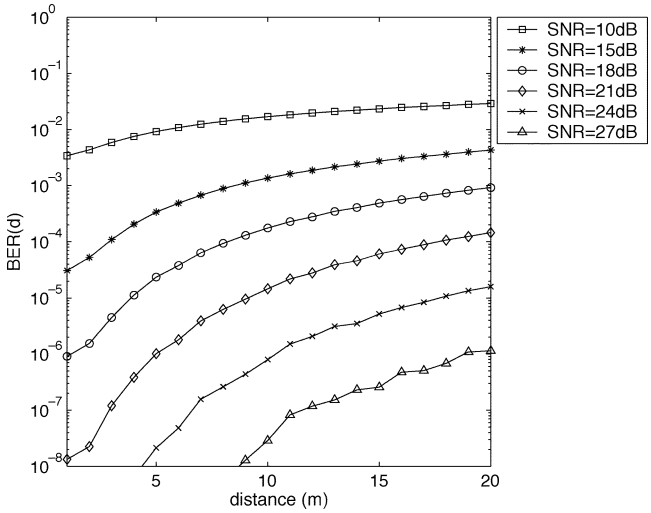

Fig. 2. The $\mathrm{BER}(d)$ vs. distance for LOS case.

every d, the channel effects are averaged over 500 000 channel realizations.[1]

Fig. 1 shows the variance estimator [16]

$$\mathrm{VAR}\left[E_s(d)\right] \simeq \frac{1}{M-1}\sum_{i=1}^{M}\left(E_{s,i}(d) - \frac{1}{M}\sum_{i=1}^{M}E_{s,i}(d)\right)^2$$

of the received energy $E_s(d)$ plotted against d.

Figs. 2 and 3 show $\mathrm{BER}(d)$ in (5) vs. d for $\mathrm{SNR} = 10$, 15, 18, 21, 24, and 27 dB, for the LOS and NLS cases, respectively. From the constant-SNR curves in Figs. 2 and 3 we can calculate the values of $\mathrm{FM}(d)$ for a fixed value of BER. Recall that $\mathrm{FM}(d) = \mathrm{SNR}(d) - \mathrm{SNR}_{\mathrm{AWGN}}$, where $\mathrm{SNR}(d)$ and $\mathrm{SNR}_{\mathrm{AWGN}}$ are the SNR values to achieve the desired BER in the multipath and AWGN channels, respectively.

As an example, remember that for an AWGN channel with orthogonal signals, we can get $\mathrm{BER} = 10^{-6}$ with $\mathrm{SNR}_{\mathrm{AWGN}} \simeq 13.5$ dB, and $\mathrm{BER} = 10^{-3}$ with $\mathrm{SNR}_{\mathrm{AWGN}} \simeq 6.5$ dB [15]. Tables I and II show the fading margin results for the LOS case,

[1]In our simulation we normalized each received pulse energy in such a way that the average received energy correspond to the value predicted by the PL for that particular d.

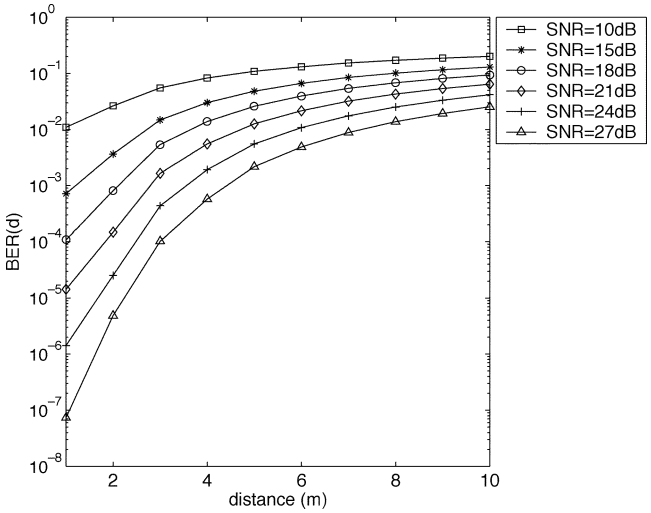

Fig. 3. The $\mathrm{BER}(d)$ vs. distance for NLS case.

TABLE I
FADING MARGIN EXAMPLE FOR LOS CASE IN FIG. 2 WITH BER 10^{-3}

d (m)	$\mathrm{SNR}(d)$ (dB)	$\mathrm{SNR}_{\mathrm{AWGN}}$ (dB)	$\mathrm{FM}(d)$ (dB)
1	$\simeq 10$	6.5	$\simeq 3.5$
10	15	6.5	8.5
20	$\simeq 18$	6.5	$\simeq 11.5$

TABLE II
FADING MARGIN EXAMPLE FOR LOS CASE IN FIG. 2 WITH BER 10^{-6}

d (m)	$\mathrm{SNR}(d)$ (dB)	$\mathrm{SNR}_{\mathrm{AWGN}}$ (dB)	$\mathrm{FM}(d)$ (dB)
1	18	13.5	4.5
5	21	13.5	7.5
10	24	13.5	10.5
20	27	13.5	13.5

TABLE III
FADING MARGIN EXAMPLE FOR NLS CASE IN FIG. 3 WITH BER 10^{-3}

d (m)	$\mathrm{SNR}(d)$ (dB)	$\mathrm{SNR}_{\mathrm{AWGN}}$ (dB)	$\mathrm{FM}(d)$ (dB)
1	15	6.5	8.5
2	18	6.5	11.5
3	21	6.5	14.5
4	24	6.5	17.5
5	27	6.5	20.5

TABLE IV
FADING MARGIN EXAMPLE FOR NLS CASE IN FIG. 3 WITH BER 10^{-6}

d (m)	$\mathrm{SNR}(d)$ (dB)	$\mathrm{SNR}_{\mathrm{AWGN}}$ (dB)	$\mathrm{FM}(d)$ (dB)
1	24	13.5	11.5
2	$\simeq 27$	13.5	$\simeq 14.5$

and Tables III and IV show the fading margin results for the NLOS case.

V. DISCUSSION AND CONCLUSIONS

Fig. 1 shows $\mathrm{VAR}[E_s(d)]$ against d. As expected, $\mathrm{VAR}[E_s(d)]$ increases as d increases.

The explanation to this phenomenon is that signals traveling longer distances experience more fading effects than those traveling shorter distances.

In general, signals traveling longer distances have a lower mean received energy because they are attenuated within

traveling distance. They also exhibit higher received energy variance because the density of the multipath increases with time (i.e., multipath replicas received earlier come back after several bounces as new, more attenuated, and further delayed reflections).

Actually, the parameters of the channel model have higher variances for higher distances; thus, as the distance increases, the received energy variation increases too. As mentioned before, the two sources of distance-dependence variations are the small scale statistics (more specifically, the variance of the filter excitation and the initial conditions in the AR channel model); and the shadow fading effects (considered in the log-normal random variable of the PL model). Currently [17] the PL model used for wireless personal area networks incorporate a "deterministic" PL model. Hence, we can expect this late model to be optimistic since shadowing effects in the PL are not taken into account.

Figs. 2 and 3 show $\mathrm{BER}(d)$ vs. d for different SNR for both LOS and NLS cases. The performance of the system suffers degradation for larger d even for fixed average SNR (this fixed average SNR being a form of average power control in the transmitter). For example, Fig. 2 shows that an average SNR fixed to 18 dB can result in BER values in the rage 10^{-6} to above 10^{-4} depending on the distance. From these results we can conclude that the power control mechanisms based on signal quality (e.g. power control based on either "instantaneous" or average carrier-to-interference ratios) are in general less effective than the criteria based on frequency of errors (e.g., power control based on BER or packet error rate).

As expected, we can see that the LOS case can achieve lower values in both BER and FM than the NLS case for a similar distance. Clearly, the NLS case exhibits a high FM increase as a function of distance. The results in Fig. 2 suggest that low power *uncoded* UWB systems can operate in a range of about 10 m under LOS conditions. Also, the results in Fig. 3 suggest that low power *coded* UWB systems could operate in a range of about 5 meters under NLOS conditions.

These results correspond to the performance of a UWB system, analyzed over a realistic, multipath residential channel. In our results we included impairments such as small scale fading produced by the multipath environment, as well as large scale fading with the PL model.

APPENDIX
CHANNEL DESCRIPTION

A. Channel Frequency Response

The channel frequency response $H(\omega)$, $w = 2\pi f$, used in (3) corresponds to the output sequence of an infinite impulse response (IIR) filter

$$H(f_i, d) = n_i - a[1]H(f_{i-1}, d) - a[2]H(f_{i-2}, d). \qquad (7)$$

The $H(f_i, d)$ is the frequency response at the frequency sample points $f_i = f_0 + (i-1)f_s$, where f_0 is the initial frequency sample point, f_s is the frequency sampling separation, and $i = 1, 2, \ldots, N_p$.

The n_i is the white noise input sequence. This noise input sequence has complex elements with real and imaginary parts that are independent and normally-distributed with zero mean and standard deviation σ, and $a[1]$ and $a[2]$ are the filter coefficients.

The output sequence of the filter gives the frequency response of the model $H(f_i, d)$. This IIR filter is fully characterized by five parameters

- The standard deviation σ of the white noise sequence n_i.
- The model coefficients $a[1]$, and $a[2]$, which are complex numbers.
- The IIR filter initial conditions given by w_0, and w_1, which are also complex numbers.

In order to obtain the channel frequency response $H(f_i, d)$ for a given d, we first obtain the standard deviation σ of the white noise sequence n_i, then n_i is generated according to the value of σ just obtained. Secondly, the filter coefficients $a[1]$, and $a[2]$ are generated. In the third step the filter initial conditions w_0, and w_1 are generated for the given d. Finally, the channel frequency response $H(f_i, d)$ is obtained as the output sequence of the IIR filter with input sequence n_i, filter coefficients $a[1]$, and $a[2]$, and initial conditions w_0, and w_1.

Here we just give a brief description of the parameters. For a full description of the distribution of the parameters needed to simulate the channel frequency response we refer the reader to [12] and [14].

The standard deviation of the input noise sequence n_i has lognormal distribution with mean and standard deviation (STD) given by

$$\begin{aligned}
\mathrm{MEAN}\left[20\log 10\left(\sigma(d)\right)\right]_{\mathrm{LOS}} &= -10.8\log 10(d) - 77.2\\
\mathrm{STD}\left[20\log 10\left(\sigma(d)\right)\right]_{\mathrm{LOS}} &= 3.7\\
\mathrm{MEAN}\left[20\log 10\left(\sigma(d)\right)\right]_{\mathrm{NLS}} &= -20.1\log 10(d) - 78.5\\
\mathrm{STD}\left[20\log 10\left(\sigma(d)\right)\right]_{\mathrm{NLS}} &= 4.5.
\end{aligned}$$

For the LOS case the coefficients magnitudes are estimated according to

$$|a[1]|_{\mathrm{LOS}} = -0.9235W + 0.3836N + 1.7869 \qquad (8)$$

and for the NLS case the coefficients magnitudes are estimated according to

$$|a[1]|_{\mathrm{NLS}} = -0.863W + 0.501N + 1.5369 \qquad (9)$$

where W has the Weibull probability distribution [18], defined by

$$f(W) = \frac{\beta}{\eta}\left(\frac{W}{\eta}\right)^{\beta-1} e^{-\left(\frac{W}{\eta}\right)^{\beta}}$$

with $\eta_{\mathrm{LOS}} = 15.191$, $\beta_{\mathrm{LOS}} = 1.312$; and $\eta_{\mathrm{NLS}} = 8.104$ with $\beta_{\mathrm{NLS}} = 1.442$.

The N in (8) and (9) is a zero-mean normal random variable with standard deviation $\sigma_{\mathrm{LOS}} = 0.0202$, $\sigma_{\mathrm{NLS}} = 0.0234$.

The distribution of the angle values $\angle a[1]_{\mathrm{LOS}}$ is Weibull, in the range of (1.95, 2.97) radians with parameters $\eta = 0.3773$ and $\beta = 16.5023$; while the distribution of $\angle a[1]_{\mathrm{NLS}}$ is also Weibull, in the range of (1.24, 2.85) radians with parameters $\eta = 0.001$ and $\beta = 7.8896$.

Once $|a[1]|$ and $\angle a[1]$ are obtained we can use linear relationships to estimate $|a[2]|$ and $\angle a[2]$

$$\begin{aligned}
|a[2]|_{\mathrm{LOS}} &= 0.1993 + 0.3908\,|a[1]|_{\mathrm{LOS}}\\
|a[2]|_{\mathrm{NLS}} &= -0.1345 + 0.5678\,|a[1]|_{\mathrm{NLS}}
\end{aligned}$$

and

$$\angle a[2]_{\mathrm{LOS}} = -6.4422 + 2.0505\angle a[1]_{\mathrm{LOS}}$$
$$\angle a[2]_{\mathrm{NLS}} = -6.5595 + 2.1022\angle a[1]_{\mathrm{NLS}}.$$

Instead of using the parameter values for η and β described before (values originally proposed in [12]), we propose alternative values (new values proposed in [14]) and use them with all previous equations

$$\eta_{\mathrm{LOS}} = 0.18 \text{ and } \beta_{\mathrm{LOS}} = 2.2 \text{ for use with (8)}$$
$$\eta_{\mathrm{NLS}} = 0.25 \text{ and } \beta_{\mathrm{NLS}} = 2 \text{ for use with (10)}$$
$$\eta_{\mathrm{LOS}} = 2.4 \text{ and } \beta_{\mathrm{LOS}} = 31 \text{ to obtain } \angle a[1]_{\mathrm{LOS}}$$
$$\eta_{\mathrm{NLS}} = 2.4 \text{ and } \beta_{\mathrm{NLS}} = 10 \text{ to obtain } \angle a[1]_{\mathrm{NLS}}.$$

Besides these new parameters, we propose to modify (9) to

$$|a[1]|_{\mathrm{NLS}} = -0.863W + 0.501N + 1.7869. \quad (10)$$

The relationship for magnitudes and phases of the initial conditions for the LOS and NLS cases are

$$|w_1|_{LOS} = 0.89|w_0|_{LOS} \quad (11)$$
$$\phi_{1LOS} = 0.9888\phi_{0LOS} + 2.26 + v_{LOS} \quad (12)$$
$$|w_1|_{NLS} = 0.93|w_0|_{NLS} \quad (13)$$
$$\phi_{1NLS} = 0.9827\phi_{0NLS} + 2.01 + v_{NLS} \quad (14)$$

where ϕ_i for $i = 0, 1$ is the phase of w_i, v_{LOS} represents a variation to the linear relationship between both initial condition phases (ϕ_{0LOS} and ϕ_{1LOS}) in the LOS case, while v_{LOS} represents the same variation in the NLS case.

The magnitudes have lognormal distribution with means and standard deviation of their logarithm value equal to

$$\mathrm{E}\left[20\log_{10}|w_0(d)|\right]_{LOS} = -16.3\log_{10}(d) - 47.9 \quad (15)$$
$$\mathrm{STD}\left[20\log_{10}|w_0(d)|\right]_{LOS} = 5.6 \quad (16)$$
$$\mathrm{E}\left[20\log_{10}|w_0(d)|\right]_{NLS} = -36.5\log_{10}(d) - 45.9 \quad (17)$$
$$\mathrm{STD}\left[20\log_{10}|w_0(d)|\right]_{NLS} = 7.8. \quad (18)$$

ϕ_{0LOS} and ϕ_{0NLS} are uniformly distributed within the interval $(-\pi, \pi)$. $v_{LOS} \sim N(0.0142, 0.294)$[2] and $v_{NLS} \sim N(0.0594, 0.4277)$.

B. Path Loss Model

The work in [13] describes a PL model derived from the same experiments used for the AR channel modeling we just described.

The PL in dB as a function of the separation distance d in meters between transmitter and receiver is given by

$$\mathrm{PL}(d) = \mathrm{PL}_0 + 10\alpha\log_{10}(d) + S \quad (19)$$

where PL_0 is the PL in dB at the reference distance of 1 m, α is the PL exponent, and S is the lognormal shadow fading in dB with standard deviation σ_s. Table V shows the parameters needed to calculate the PL in (19).

[2] $X \sim N(m, std)$ means X is a random variable normally distributed with mean m and standard deviation std.

TABLE V
PL PARAMETER VALUES. THE $N(\mathrm{MEAN}, \mathrm{STD})$ DENOTES THE GAUSSIAN DISTRIBUTION

	$\mathrm{PL}_0(dB)$	α	σ_s
LOS	47	$\sim N(1.7, 0.3)$	$\sim N(1.6, 0.5)$
NLS	51	$\sim N(3.5, 0.97)$	$\sim N(2.7, 0.98)$

ACKNOWLEDGMENT

The authors thank the constructive and enriching comments provided in the reviewing process.

REFERENCES

[1] R. A. Scholtz, "Multiple access with time hopping impulse modulation," in *Proc. IEEE MILCOM Conf.*, 1993, invited paper, pp. 447–450.
[2] F. Ramírez-Mireles and R. A. Scholtz, "Performance of equicorrelated ultra-wideband pulse-position-modulated signals in the indoor wireless impulse radio channel," in *Proc. IEEE PACRIM'97*, vol. 2, Aug. 1997, pp. 640–644.
[3] *IEEE J. Select. Areas Commun.*, vol. 20, no. 9, Dec. 2002. Special Issue on "Ultra-wideband radio in multi-access wireless communications".
[4] D. Gerakoulis and P. Salmi, "Link performance of an ultra wide bandwidth wireless in-home network," in *Proc. Int. Symp. Computers and Commun.*, 2002, pp. 699–704.
[5] S. Roy, J. R. Foerster, V. S. Somayazulu, and D. G. Leeper, "Ultrawideband radio design: the promise of high-speed, short-range wireless connectivity," *Proc. IEEE*, vol. 92, no. 2, pp. 295–311, Feb. 2004.
[6] U.S. Federal Communications Commission, First Report and Order for UWB Technology, U.S. Federal Communications Commission, Apr. 2002.
[7] F. Ramírez-Mireles, M. Z. Win, and R. A. Scholtz, "Performance of ultra-wideband time-shift-modulated signals in the indoor wireless impulse radio channel," in *Proc. 31st Asilomar Conf. Signals, Systems, and Computers*, vol. 1, Nov. 1997, pp. 192–196.
[8] F. Ramírez-Mireles, "On the performance of ultra-wide-band signals in Gaussian noise and dense multipath," *IEEE Trans. Veh. Technol.*, vol. 50, no. 1, pp. 244–249, Jan. 2001.
[9] D. Cassioli, M. Z. Win, F. Vatalaro, and A. F. Molish, "Performance of low-complexity rake reception in a realistic UWB channel," in *Proc. IEEE ICC'02*, vol. 2, Mar. 2002, pp. 763–767.
[10] K. Pahlavan and A. H. Levesque, *Wireless Information Networks*. New York: John Wiley and Sons, 1995, p. 241.
[11] R. Bastidas-Puga, F. Ramírez-Mireles, and D. Muñoz-Rodríguez, "Performance of UWB PPM in residential multipath environments," in *Proc. IEEE Veh. Technol. Conf. 2003 Fall*, Oct. 2003.
[12] W. Turin, R. Jana, S. Ghassemzadeh, C. Rice, and V. Tarokh, "Autoregressive modeling of an indoor UWB channel," in *Digest of Papers UWBST'02 Conf.*, May 2002, pp. 71–74.
[13] S. Ghassemzadeh, R. Jana, C. Rice, W. Turin, and V. Tarokh, "A statistical path loss model for in-home UWB channel," in *Digest of Papers UWBST'02 Conf.*, May 2002, pp. 59–64.
[14] R. Bastidas-Puga, "Analysis of Multipath Performance of UWB Systems Using an Autoregressive Channel Modeling," M.Sc. thesis in E.E., Div. of Electronics, Computer, Information and Communications, ITESM, Jan. 2003.
[15] R. M. Gagliardi, *Introduction to Telecommunications Engineering*. New York: John Wiley and Sons, 1988, pp. 357–437.
[16] A. Leon-Garcia, *Probability of Random Processes for Electrical Engineering*: Addison-Wesley, May 1994.
[17] A. F. Molish, J. R. Foerster, and M. Pendergrass, "Channel models for ultrawideband personal area networks," *IEEE Wireless Commun.*, vol. 10, no. 6, pp. 14–21, Dec. 2003.
[18] K. Bury, *Statistical Distributions in Engineering*, 1st ed: Cambidge University Press, 1999.